Astron. Astrophys. 322, 234–241 (1997)

ASTRONOMY
AND
ASTROPHYSICS

Abundance analysis of roAp stars

III. γ Equulei*

T.A. Ryabchikova[1], **S.J. Adelman**[2,3], **W.W. Weiss**[4], **and R. Kuschnig**[4]

[1] Institute for Astronomy, Russian Academy of Sciences, Pyatnitskaya 48, 109017 Moscow, Russia (ryabchik@inasan.rssi.ru)
[2] Department of Physics, The Citadel, 171 Moultrie Street, Charleston, SC 29409, USA (adelmans@citadel.edu)
[3] Guest Investigator, Dominion Astrophysical Observatory
[4] Institute for Astronomy, Univ. Vienna, Türkenschanzstr. 17, A-1180 Vienna, Austria (last_name@galileo.ast.univie.ac.at)

Received 7 October 1996 / Accepted 18 November 1996

Abstract. A spectroscopic analysis of the rapidly oscillating chemically peculiar star γ Equ yields $T_{\rm eff} = 7700$ K, log $g = 4.20$, a microturbulence and $v \cdot \sin i$ which cannot be determined reliably, but which must be close to zero, because line broadening can be modelled by magnetic field effects alone. A mean magnetic field modulus of B = 4.0 kG is estimated by comparing synthetic Zeeman pattern with observations. This value provides another phase point for magnetic field variations of γ Equ, a CP2 star with the longest hitherto known magnetic field period of about 77 years. For a simple dipolar field geometry, the angle between the line of sight and the magnetic axis ≈ 130 deg (*or* ≈ 50 deg).

We discuss in some detail the problems for abundance determinations in the presence of a strong magnetic field and we increase substantially the number of ions to 42, for which abundances are now available. In particular, we obtain a more reliable abundance of $\log(\mathrm{Eu/N}_{tot}) = -10.24$, and find Fe and the light elements, C to Ca, to have nearly solar abundances. Co is clearly overabundant, and Nb and Mo are the most overabundant elements in γ Equ relative to the Sun.

Key words: stars: abundances; chemically peculiar; magnetic field; oscillations; individual (γ Equ)

1. Introduction

γ Equ (HD 201601, HR 8097, mag(V) = 4.69) is a very sharp-lined chemically peculiar star of spectral class near F0 V. It is remarkable also as a member of the rapidly oscillating CP2 (roAp) stars. Kurtz (1983) discovered oscillations with a period of 12.44 min and an amplitude in Johnson B which was variable between 0.5 and 1.5 mmag from night to night. The most recent photometric investigation of pulsation frequencies (Martinez et al. 1996) presents evidence for p–modes with four frequencies which are roughly spaced by about 30μHz. The authors interprete the data as alternating even and odd ℓ–modes for a slightly evolved A-type star. From radial velocity time series of γ Equ, Libbrecht (1988) was able to determine two frequencies, both of which were later confirmed by data obtained during a photometric multi-site campaign (Martinez et al. 1996). The small RV amplitude of 42 ms^{-1} found by Libbrecht explains why earlier similar attempts using smaller telescopes at ESO failed (Schneider & Weiss 1989).

The main purpose of our series of papers on the abundance analyses of roAp stars is to provide accurate fundamental parameters of this group of pulsating stars, especially $T_{\rm eff}$, log g and abundances. These parameters are important boundary values for selecting stellar models used in the context of asteroseismology.

Zeeman observations from the early 1950's (Babcock & Cowling 1953) to the late 1980's (Mathys 1991) showed a longitudinal magnetic field which slowly decreased from +500 G to -1000 G. Bonsack & Pilachovski (1974) proposed a 72-year magnetic period for γ Equ which is supported by Leroy et al. (1994) on the basis of polarimetry. A sine fit to all published longitudinal magnetic field values by the same authors results in a period of 77 ± 10 yr, which makes γ Equ the slowest known rotator among the CP stars. A rigidly rotating F0 star with a 77 yr rotation period has a $v_{\rm equ} = 0.003$ km s^{-1}, which presently cannot be confirmed even with the highest spectral resolution available to us. However, most spectral lines in γ Equ appear to be broadened, and all published estimates for $v_{\rm equ}$ range between $v_{\rm equ} < 3$ km s^{-1} (Preston 1971) to $v_{\rm equ} = 8$ km s^{-1} (Renson, Kobi & North 1991). In this paper we investigate also to what extent this additional line broadening is caused by a magnetic field.

Send offprint requests to: Werner W. Weiss

* Based on observations obtained at the European Southern Observatory (La Silla, Chile), Dominion Astrophysical Observatory, Observatoire de Haute-Provence, and at the Crimean Astrophysical Observatory

Scholz (1979) was the first to report a probable detection of a resolved Zeeman pattern. His result was confirmed by Mathys (1990) who obtained a lower limit of 3.6 kG for the mean magnetic field modulus from the resolved Fe II λ6149.2 Å line which has a simple doublet Zeeman structure. Mathys & Lanz (1992) obtained evidence for a gradual increase of the mean magnetic field modulus for γ Equ from 3.7 kG (May 1988) to 4.0 kG (Oct. 1990).

A magnetic field affects spectral line equivalent widths through the magnetic intensification. Landi Degl'Innocenti (1975) showed that the combined effect of the magnetic and hyperfine-structure splitting on the abundance determination for the Eu II λ4205 Å line may be as large as +1.5 dex for a magnetic field of 3 kG. This sensitivity may partially explain why abundances of Rare Earth elements (REE) in CP stars often exceed the solar values by more than 2.0 dex.

The most detailed abundance study of γ Equ was published by Adelman (1973). He derived abundances for 22 chemical elements and he took into account the influence of a magnetic field of 1.8 kG (Preston 1971) on his abundance determinations by allowing for a magnetic pseudo-microturbulence which is different for each spectral line. For some REE Adelman obtained overabundances relative to the Sun of 2.5 dex (Sm) and up to 3.2 dex (Eu). Magazzu & Cowley (1986) carefully repeated the analysis and found significantly lower overadundance factors which did not exceed 1.5 dex for Eu and Gd. They also found the abundances of the light and intermediate REE in γ Equ to be comparable to cool Ap stars and to the Am star 32 Aqr.

All published abundance and line profile studies were based on relatively high resolution photographic spectra, but with a signal-to-noise ratio less than 80. Our investigation is a careful investigation of line profiles in γ Equ using linear detectors and high resolution, high S/N spectra, in order to search for line broadening due to a magnetic field. Furthermore, we present an abundance analysis which is based on a fully blanketed ATLAS9 model atmosphere and on critically assessed atomic line parameters.

2. Observations

In Table 1 we present a log of our observations and list the mid-time of the exposures, the wavelength regions observed, the signal-to-noise ratios for typical continuum pixels, the average full-width-at-half-maximum (FWHM) of the slit transfer functions, and the observatory. The FWHM value corresponds to the theoretical resolutions, where the real one may be less due to non-optimal focussing.

European Southern Observatory (ESO): Spectrum No.1 is based on an average of six frames obtained with the ESO coudé echelle spectrograph which was fed by the coudé auxiliary telescope. This configuration included the long focus Maksutov camera system and a 1024 x 640 thinned, backside illuminated RCA-CCD detector, resulting in a reciprocal linear dispersion of 1.45 Åmm^{-1} at 5000 Å. The spectra were obtained as part of a program to detect line profile variations in roAp stars, caused by pulsation. The program stars were trailed along the slit so that time resolved spectroscopy was possible by analyzing spectra extracted from individual CCD lines (Rogl 1996). One frame typically contains 42 well exposed lines. After the standard reduction steps (bias subtraction, flat fielding, wavelength calibration) we computed for each frame a mean stellar spectrum from these 42 lines. The average spectrum from the best frames was used for this paper.

Table 1. Log of our γ Equ observations. S/N: signal-to-noise ratio of a typical continuum pixel, FWHM: spectral resolution in mÅ.

No.	Mid exposure JD 2440000+	Range Å	S/N	FWHM mÅ	Obs.
1	7741.889	4266–4285	150	50	ESO
2	9280.677	3882–3942	150	90	DAO
3	7750.847	4158–4225	150	90	DAO
4	9618.792	4210–4277	150	90	DAO
5	8845.818	4651–4717	200	90	DAO
6	8940.603	4706–4772	200	90	DAO
7	8154.286	4390–4602	150	300	OHP
8	8155.000	6127–6155	200	200	CrAO

Dominion Astrophysical Observatory (DAO): Spectra No.2 to 6 were obtained with the long camera of the coudé spectrograph of the 1.22-m telescope which was equipped with a 1832 element Reticon detector with 15 μ wide pixels. Each exposure was flat-fielded with a tungsten lamp placed in the coudé mirror train. A stop in the center of the collimated light beam simulated the vignetting effect by the secondary telescope mirror.

Observatoire de Haute-Provence (OHP): Spectrum No.7 was obtained in Sept. 1990 with the AURELIE spectrograph of the Observatoire de Haute-Provence and a linear 2048 pixel CCD array detector. The data were reduced with IHAP at the ESO headquarter in Garching and 'final touches' were given in Vienna with a PC-based spectrum reduction package, SPE, written by S. Sergeev of the Crimean Astrophysical Observatory.

Crimean Astrophysical Observatory (CrAO): Spectrum No.8 is an average of three spectra obtained in September 17-22, 1990, with the first camera of the coudé spectrograph of the Crimean 2.6-m telescope, equiped with a CCD detector.

3. Data reduction

Normalisation to the continuum was done for all spectra with the PCIPS package (Smirnov & Piskunov 1994). First, we calculated synthetic spectra for each spectral band (without Hydrogen lines) with the preliminary abundances of γ Equ obtained by Kupka et al. (1995), and determined spectral regions with an undisturbed continuum. These regions were identified in the observed spectrum and a polynomial fit of typically 3rd order computed, in the hydrogen line wings of 5th order. This fit was used for normalizing the spectra.

The consistency of this procedure can be judged by comparing overlapping regions of normalized spectra obtained with dif-

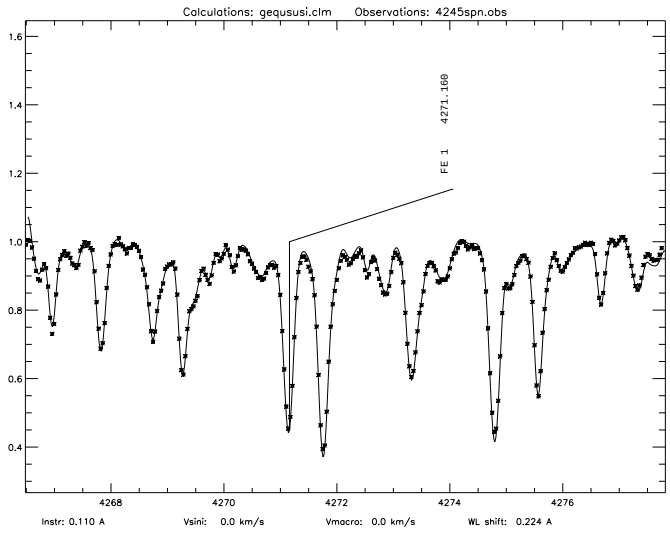

Fig. 1. Comparison of the DAO spectrum (asterisks) with the CAT-CES spectrum (full line) which is folded with a Gaussian profile (FWHM = 0.11 Å) for a better comparison with the DAO observations which have lower spectral resolution.

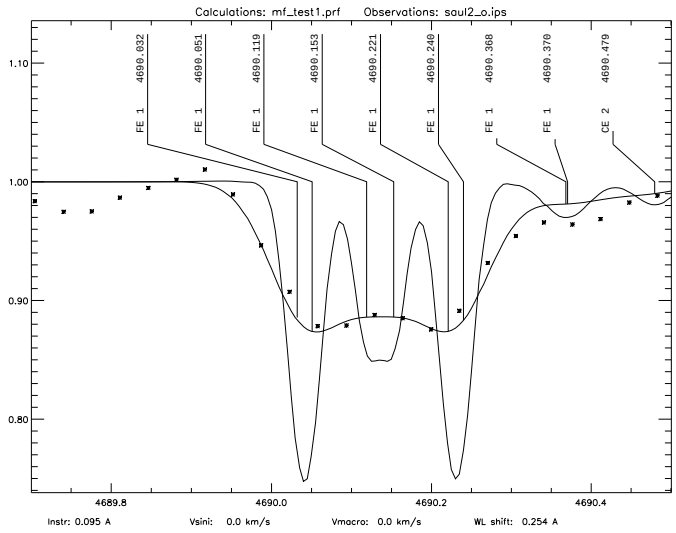

Fig. 2. Fe I λ 4690 Å line (spectrum No.5, see Table 1). Comparison of the observed (asterisks) and synthesized line profiles (heavy line) for magnetically sensitive spectral lines ($\phi \approx 130^\circ$). The synthetic spectrum is shown with as a thin line, without instrumental broadening.

ferent instrumentation (Fig. 1). An additional broadening with a Gaussian profile with a FWHM = 0.11 Å was applied to the ESO spectrum for a better comparison with the DAO data.

Wavelengths and equivalent widths were measured with the Multi-Profile program (Smirnov & Ryabchikova 1995) which simultaneously fits Gaussian profiles to the metal lines. A linear least-squares fit of our equivalent widths in mÅ to those 48 lines we have in common with Adelman (1973) resulted in:

$$W_{\text{this paper}} = (1.039 \pm 0.029) \cdot W_{\text{Adelman}} - (2.178 \pm 2.094)$$

The relatively large dispersion of 7.7 mÅ around the regression line is caused by severe blending of magnetically broadened lines and the lower signal-to-noise ratio of the Palomar Observatory spectrogram that Adelman used.

A similar relation between the measurements by Magazzu & Cowley (1986) and ours, unfortunately, cannot be determined, because we have only five unblended lines in common, for which, however, the agreement is quite good. For five blended lines the equivalent widths measured by Magazzu & Cowley are systematically smaller.

The Vienna Atomic Line Database (VALD, Piskunov et al. 1995) was extensively used for line identifications, based on preliminary abundances obtained by Kupka et al. (1995) as initial parameters for the line selection procedure. Only those lines from VALD were considered for our synthesis which contribute without any broadening at least 1 % of the continuum level to the spectrum. Lines of all neutral and singly-ionized elements identified by Adelman (1973) and by Adelman et al. (1979) are present in our spectra, except of Rh I, Pd I, U II and a few Rare Earth elements, which might be caused by differences in the wavelength coverage of the respective observations.

A more detailed description of the identification of various ions will be given in Sec. 6. Radial velocity measurements derived from DAO spectra resulted in RV = -15.8$\pm$0.45 km s^{-1}. Mathys (1990) obtained RV = -17.0 km s^{-1}, while Beavers & Eitter (1986) measured RV = -14.5 km s^{-1}. The differences between these radial velocity values are larger than the formal errors and they might indicate the presence of a stellar companion or instrumental systematics.

4. The model atmosphere

A detailed description of the choice of model atmosphere parameters and the abundance analysis method is given in the first two papers of this series (Kupka et al. 1996, hereafter Paper I, and Gelbmann et al. 1996, Paper II). In the literature we found effective temperature values in a narrow range from 7500–8100 K. Adelman et al. (1995) obtained the best simultaneous fit to the optical spectrophotometric data and the H_γ line profile for a 0.5 dex metal overabundant model with $T_{\rm eff}$ = 7700 K, log g = 4.2 and $\xi_{\rm t}$ = 2 km s^{-1}, which agrees with the results obtained from our preliminary abundance analysis (Kupka et al. 1995): $T_{\rm eff}$=7750 K, log g=4.0, $\xi_{\rm t}$=1 km s^{-1}.

The determination of stellar temperature and surface gravity by using Strömgren $uvby - \beta$ photometry appears to yield good estimates for the normal B, A, and F stars. However, the energy distributions of chemically peculiar stars exhibit greater line blanketing and broad continuum features which make the use of such methods more problematic. When one tries to determine the effective temperature and surface gravity of stars with parameters similar to those of γ Equ by matching optical spectrophotometric fluxes and Balmer line profiles with the predictions from ATLAS9 models one finds that both the metallicity and the microturbulence have small, yet measurable effects. Both factors affect the line blanketing and the redistribution of the flux from the ultraviolet to the optical region. The magnetic

Table 2. Zeeman configuration for some spectral lines used in our analysis (Beckers 1969) and the resulting magnetic field (last column) derived from our observations. The π component splittings are followed by a relative intensity given between '<>', the σ components are followed by relative intensities between '()'

element	λ (Å)	Transition	Zeeman pattern	B (kG)
Fe II	4273.326	$^4P_{3/2} - ^4D^0_{1/2}$	0.87< 1000 >0.87(250)2.60(750)	4.2
Fe I	4273.869	$^3P_1 - ^5P^0_2$	0.00< 800 > 0.33 < 600 >1.50(100)1.83(300)2.17(600)	4.3
Fe I	4690.136	$^5P^0_1 - ^7D_1$	0.50< 1000 >2.50(500)3.00(500)	3.4
Fe I	4704.954	$^5P^0_1 - ^7D_0$	0.00< 2000 >2.50(1000)	4.2
Fe I	4710.285	$^3G_3 - ^3G^0_3$	0.00< 2000 >0.75(1000)	3.5-4.0

field of γ Equ acts similarly, but its detailed behavior is not identical with those of microturbulence and metallicity. Furthermore, we used scaled solar metallicity models and γ Equ's abundances are most likely somewhat different. The effects of this latter factor can be tested using opacity sampling model atmospheres codes such as ATLAS12 when it becomes available. However, the effects of the magnetic field may be more important.

It will be shown in the following section that the intrinsic microturbulence in the atmosphere of γ Equ is close to zero. The magnetic field causes an intensification effect for any unresolved Zeeman pattern which mimics additional microturbulence (see Paper I). Our tools presently do not allow us to perform model atmosphere calculations including magnetic field broadening. Therefore we used the classical microturbulence method to approximate the magnetic field effects. A total of 61 Fe I spectral lines with an effective Landé factor ranging from 0.67 to 2.5 were chosen for the analysis. Abundance calculations with the Kurucz's program WIDTH9 gave a mean value of ξ_t close to 2 km s^{-1}. For our preliminary abundance analysis we used lines with effective Landé factors less than 1.5, which explains our smaller ξ_t. A magnetic field of 3.6 kG provides a pseudo-microturbulence of about 2.3 km s^{-1} for a 4500 Å line with $g_{eff} = 1.0$, depending on the degree of line saturation and the actual Zeeman pattern. We consider our value of ξ_t as a good approximation of the average magnetic intensification in the atmosphere of γ Equ.

5. Magnetic field and stellar rotation

A comparison of synthetic spectra with observations clearly indicate that many of the spectral lines are wider and have a more complex structure than is expected for a non–magnetic star of otherwise similar properties. A list of lines used by us for magnetic modelling including their Zeeman pattern (Beckers 1969) is given in Table 2.

For each Zeeman component we computed the corresponding shift due to a magnetic field according to:

$$\Delta\lambda_{\rm magn} = 4.66 \cdot 10^{-13} \cdot \lambda^2 \cdot g \cdot B_{\rm mean}, \quad (1)$$

where $\Delta\lambda$ is the wavelength shift in Å, g is the Landé factor of the component, and B is the magnetic field strength in Gauss.

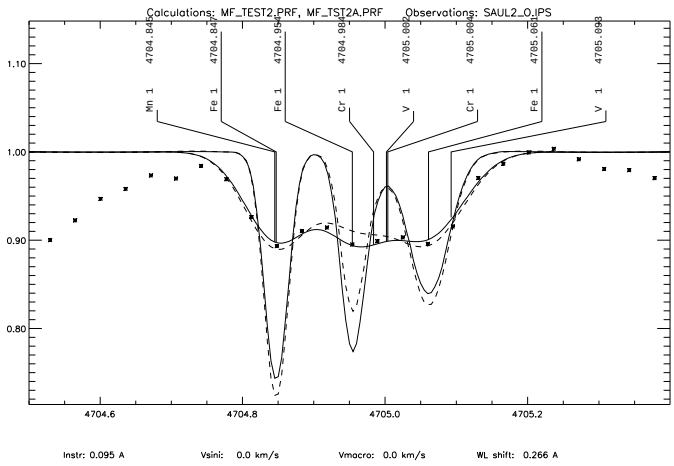

Fig. 3. Fe I λ 4705 Å line (spectrum No.5, see Table 1 and Fig. 2 for explanations). The dashed line is a synthesized spectrum with an intensity ratio of 0.6 for the π and $\sigma_\pm$ components ($\phi \approx 120^\circ$).

The relative intensities of the π and σ components are given according to Seares (1913):

$$I_\pi = I^0_\pi \cdot \sin^2\phi, \quad \text{and} \quad I_\sigma = I^0_\sigma \cdot (1 + \cos^2\phi), \quad (2)$$

where ϕ is the angle between the magnetic field vector and the line of sight.

We varied the magnetic field modulus B and the relative intensities of the π and σ components to obtain the best fit to the observed line profiles. I^0_π and I^0_σ were taken from Beckers (1969, see Table 2). The resulting line profile is the sum of all Zeeman components, where the integration was done for line opacity coefficients. Each of the Zeeman components was shifted according to formula (1) and its gf-value was assumed proportional to the relative intensity in theoretical pattern. The sum of all gf-values of the Zeeman components is equal to the gf-value of the unsplitted line. For each investigated spectral feature we obtained the best solution for a ratio of 0.84 for the intensities of the π and $\sigma_\pm$ components. This ratio requires $\phi \approx 130^\circ$ (or 50°) for the mean value of the angle between the magnetic field vector and the line of sight. The values of B obtained for each line are given in the last column of Table 2.

Our mean magnetic field modulus of 4.0 kG is in good agreement with Mathys & Lanz's (1992) value for the Fe II lines λ

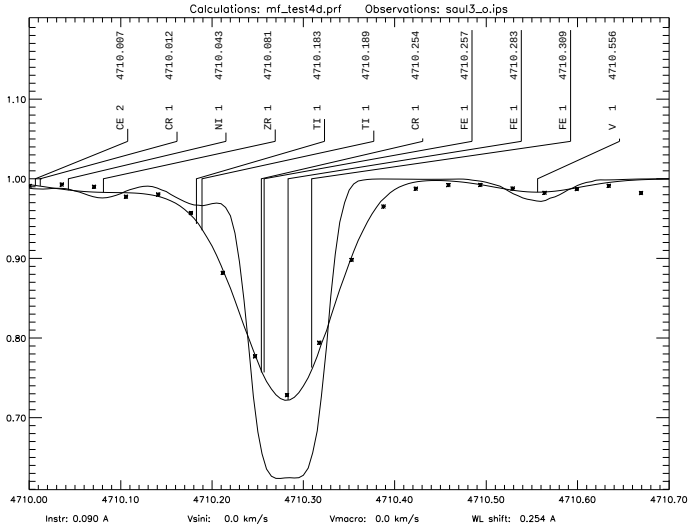

Fig. 4. Fe I λ 4710 Å line (spectrum No.6, see Table 1). See Fig. 2 for explanations.

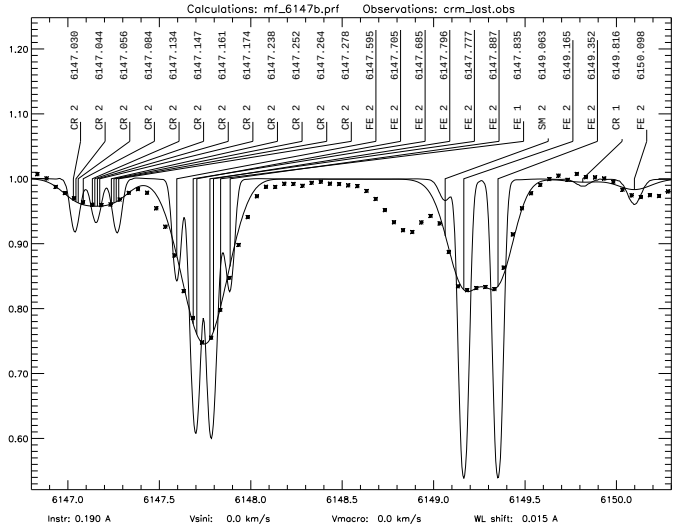

Fig. 6. Fe II λ 6148 Å and Fe I λ 6149 Å lines (spectrum No.8, see Table 1). See Fig. 2 for explanations.

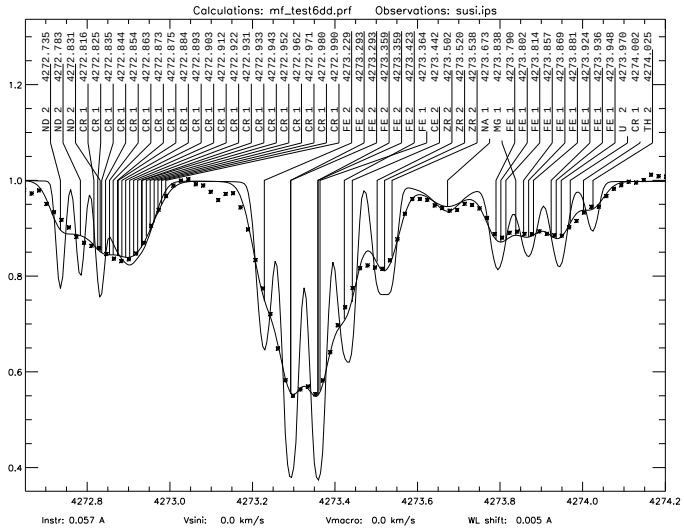

Fig. 5. Fe II λ 4273 Å and Fe I λ 4274 Å lines (spectrum No.1, see Table 1). See Fig. 2 for explanations.

6147.7 Å and λ 6149.2 Å. We did not use these lines because of the relatively low spectral resolution of our data.

The dipole model for the magnetic field geometry proposed by Leroy et al. (1994) can help us to determine the angle ϕ. They found $B_p = 5.5$ kG, $i = 150°$, and $\beta = 80°$, where β is the angle between the rotation axis and the positive magnetic pole. Our observations were obtained at phases close to the maximum negative magnetic field where the angle between the negative magnetic pole and the line of sight should be about 50° (or 130°, if we consider the vector of the negative magnetic pole) according to the model proposed by Leroy et al. (1994). Our value for the angle $\phi = 130°$ which coincides with the angle between the the line of sight and the negative magnetic pole, supports the dipolar geometry proposed for γ Equ.

The largest negative value of the mean longitudinal magnetic field B_e = -1.1 kG and the mean modulus $B = 4.0$ kG are consistent for a purely dipolar field with $\phi \approx 120°$ which is not very different from our value. However, such a ϕ-value would require a ratio of 0.6 for the intensities of the π and $\sigma_\pm$ components, which we do not observe. Part of this discrepancy may be caused by the deviation of the magnetic field configuration from a pure dipole, as it is observed for other magnetic stars (see Leroy et al. 1995), and/or a distortion of the photosphere caused by the magnetic field.

Figs. 2 to 6 show comparisons between observed and computed line profiles. We need no microturbulence nor any rotational broadening to fit our observations. Consequently, $v \cdot \sin i$ of γ Equ must be close to zero, which is compatible with a rotational period of 77 years. Obviously, the microturbulence reported in the literature is simulated by the magnetic field. In Fig. 5 we present a 1.5 Å wide spectral region of computed spectra compared with our observations taken with the CATCES instrument (set No. 1 in Table 1). All but a few weak lines were successfully synthesized with their full Zeeman patterns.

To fit the Fe II λ 4273.326 Å line with the same magnetic field parameters as are inferred from the Fe I lines, we had to change the relative intensities of the σ components to 0.87(700)2.6(300). Complex Zeeman configurations, like that for Cr I λ 4272.903 Å which has a total number of 21 components, result in a line broadening corresponding to $v_{\rm equ} = 5.7$ km s^{-1}. This also confirms that line broadening is dominated for γ Equ by the magnetic field.

6. Abundance analysis

Most of the abundance analysis was done with Kurucz's code WIDTH9. For severely blended Mg II, Nb II, Eu II and Tb II lines we used the technique described in Paper I based on spectrum synthesis. Table 3 summarizes the mean abundances for

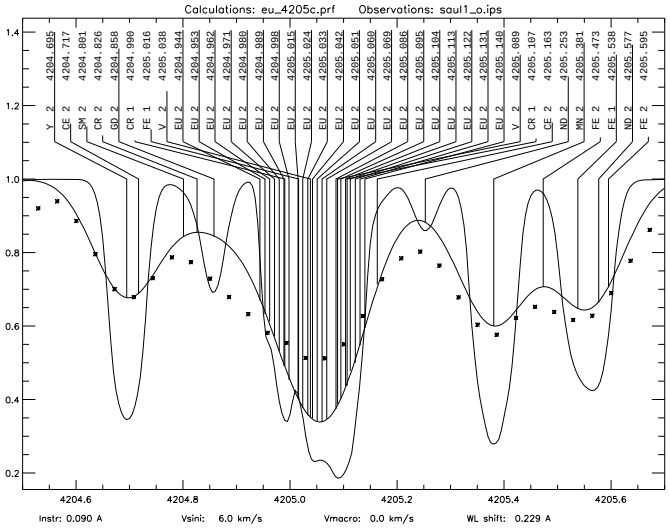

Fig. 7. Comparison of the observed (asterisks) and synthesized line profiles (heavy line) for Eu II λ 4205 Å lines (spectrum No.3, see Table 1). The full magnetic pattern (unwidened) is shown by a thin line.

all investigated ions and compares them with those of Adelman (1973), Magazzu & Cowley (1986), and with the abundances of α Cir (Kupka et al. 1996, Paper I). For comparison, we give the solar abundances (Anders & Grevesse 1989) in the last column of Table 3, complemented by recent data on CNO (Biemont et al. 1993), S (Biemont, Quinet & Zeippen 1993), Ti (Bizzarri et al. 1993), Cr (Pinnington et al 1993), Fe (Biemont et al. 1991, Holweger et al.1991), and Dy (Biemont & Löwe 1993). Individual equivalent widths and abundances will be submitted to the Strasbourg Data Center.

The elements for which the γ Equ abundances were determined by spectrum synthesis are marked with an asterisk. Abundances for α Cir and the Sun are given in the quoted references for particular elements and not for ions, and we use therefore the same abundance for ions of the same element. All oscillator strengths were extracted from VALD (Piskunov et al. 1995).

With the exception of the REE the abundances determined by Adelman (1973) are in good agreement with our results. For the REE he used Corliss & Bozman's (1962) gf-values which are now known to suffer from systematic errors. Magazzu & Cowley determined for La II a substantially smaller abundance which cannot be fully explained by differences of the gf-values used in both studies. We have one La II λ3921.54 Å line in common for which our equivalent width is larger by a factor of 1.75 than is given in Magazzu & Cowley. We presently cannot explain this discrepancy.

The Eu abundance is determined with the spectrum synthesis technique and takes into account the Zeeman configuration. The results for the Eu II λ4205.05 Å line is shown in Fig. 7. Even when taking the full Zeeman pattern into account we cannot fit the line profile sufficiently well. Some extra line broadening is needed, which might be the hyper-fine-structure splitting. We did not take this into account. Our Eu abundance can be considered therefore as an upper limit. The effects of hyperfine-

Table 3. Abundances of the roAp star γ Equ with error estimates in units of 0.01 dex based on n measured lines. An asterisk indicates that the spectrum synthesis technique was used for the abundance determination. The abundances for α Cir and the Sun are given for elements only and we quote the same abundance for ions of the same element. *References:* Adelman (1973, SA), Magazzu & Cowley (1986, MC), Kupka et al. (1996, FK)

Ion	γ Equ			α Cir	$\odot$
	log(N/N_{tot})	n	SA ; MC	FK	
C I	-3.66±38	4		-4.00	-3.47
Na I	-5.27 25	3		-5.90	-5.71
Mg I	-4.19 08	3			-4.46
Mg II*	-4.50	2	-4.62	-4.46	-4.46
Al II	-4.93:	1			-5.57
Si I	-4.42 25	4	-4.43	-4.20	-4.49
S I	-4.74 37	3			-4.71
Ca I	-5.40 22	4	-5.18	-5.15	-5.68
Ca II	-6.03:	1		...	-5.68
Sc II	-9.45 12	4	-9.47	-9.80	-8.94
Ti I	-6.95 12	7	-7.14:	-6.87	-7.00
Ti II	-7.00 22	20	-6.99	-6.87	-7.00
V I	-7.15 04	3		-7.65	-8.04
V II	-7.05 34	8	-7.27		-8.04
Cr I	-5.43 29	40	-5.36	-5.55	-6.30
Cr II	-5.66 34	15	-5.19	-5.55	-6.30
Mn I	-6.01 24	10	-6.80	-6.00	-6.49
Mn II	-5.46 19	12	-5.92	-6.00	-6.49
Fe I	-4.28 25	61	-4.03	-4.50	-4.56
Fe II	-4.42 45	10	-4.09	-4.50	-4.56
Co I	-5.98 11	4	-6.42	-5.50	-7.12
Co II	-6.18:	1		-5.50	-7.12
Ni I	-6.06 24	7	-6.11	-6.15	-5.79
Ni II	-5.49:	1			-5.79
Sr I	-6.84 21	2			-9.14
Sr II*	-7.43	1	-7.40	-7.25	-9.14
Y I	-7.94	1			-9.80
Y II	-8.51 32	6	-8.28	-8.50	-9.80
Zr II	-8.68 28	7	-8.78	-9.00	-9.44
Nb II*	-8.85:	1			-10.62
Mo II	-8.25 09	3			-10.12
Ba II	-9.06 15	2	-8.77	-10.30	-9.91
La II	-9.59 20	4	-9.02 ;-10.38	-10.32:	-10.82
Ce II	-9.20 34	24	-9.21 ; -9.19	-9.40	-10.49
Pr II	-9.98 32	5	-8.32:;	-10.40	-11.33
Nd II	-9.17 32	20	-8.96 ; -9.36	-9.30	-10.54
Sm II	-9.53 24	14	-8.40 ; -9.80	-9.50	-11.04
Eu II*	-10.24 28	2	-8.27 ;-10.01	-9.40	-11.53
Gd II	-9.35 21	5	-8.98 ; -9.47	-9.45	-10.92
Tb II*	-10.69:	2			-11.94
Dy II	-9.14 17	3		-10.00:	-10.84
Er II	-10.04 22	2			-11.11
Teff	7700		8100 ; 8000	7900	
log g	4.20		4.00 ; 4.00	4.20	

structure on the abundance of Eu II were discussed by Hartoog et al. (1974).

The time span between data set No. 1 and No. 8 of Table 1 is 1877 days which results in a phase difference of about 0.07 for a rotation period of 77 years. During our reductions we did not find evidence for smearing effects which eventually could influence our abundance analysis.

6.1. Light elements: C to Ca

All the light elements have nearly their solar abundance within the limits of our errors. Both Mg II lines at λ4428 Å and λ4481 Å are blended, and we applied therefore the spectrum synthesis technique to determine the abundance. The Al abundance is quite uncertain because a determination with the resonance line Al I λ3944 Å gives $\log(\mathrm{Al}/\mathrm{N}_{tot})$ = -6.96, which is smaller by about 2.0 dex relative to the only Al II line which can be measured in our spectra. Resonance lines are known to suffer from NLTE effects and they are not well suited for abundance analyses.

6.2. Iron peak elements: Sc to Ni

Sc is underabundant in all three roAp stars we have analyzed so far (α Cir, γ Equ, and HD 203932). On average, V and Cr are overabundant by 0.8 dex. Mn lines suffer from hyperfine-structure splitting and the smaller value of $\log(\mathrm{Mn}/\mathrm{N}_{tot})$=-6.01 derived from Mn I lines may therefore be a lower limit to the Mn abundance. Mn is overabundant by 0.5 dex in the three roAp stars. Fe is only mildly overabundant in γ Equ, if at all, and it is normal in α Cir. Co is about 1.0 dex overabundant in γ Equ, while Ni is slightly deficient. A large deviation of the relative Co:Ni and Co:Fe abundances from the solar values seems to be a common feature for roAp stars (Kupka et al. 1995, 1996). While no violation of the odd-even effect is observed in the sequence Cr-Mn-Fe, there is a tendency to its violation in the sequence Fe-Co-Ni. The significance of the large Co overabundance may be confirmed only after correction for hyperfine-structure splitting.

6.3. s-process elements: Sr to Mo and Ba

The Sr abundance derived from lines of neutral and ionized species is clearly different. VALD containes gf-values for Sr I lines taken from Corliss & Bozman (1962). Astrophysical gf-values derived from the solar spectrum (see for example Thévenin 1989) are in average larger by 0.4 dex. With this correction, the Sr I lines will give $\log(\mathrm{Sr}/\mathrm{N}_{tot})$ = -7.24, which agrees better with the value derived from Sr II λ4161 Å. The Sr abundance is similar in all roAp stars and about 0.8 dex lower in the Am star HR 178 (van't Veer-Menneret et al. 1988), while the Y and Zr abundances are similar in roAp and Am stars. A violation of the odd-even effect is observed in all roAp stars. Because the Nb abundance is derived only from a single line (Nb II λ3919.619 Å), the overabundance by 1.8 dex may be rather uncertain, but it is comparable to Mo. We used the three Mo II lines at $\lambda\lambda$3915.422, 4209.642, 4279.022 Å for our abundance determination. Nb and Mo show the largest anomalies in the spectrum of γ Equ relative to the Sun.

6.4. Rare Earth elements: La to Er

The rare-earth sequence agrees well with relative solar abundances which are enhanced by a factor of 23 (+1.36 $\pm$ 0.18 dex). Only the Dy and Er overabundances differ from the mean by about 0.35. The analyses of roAp stars are based on the same source for gf-values, while a different one was used for the abundance study of the Am star HR 178. A comparison of both sets of gf-values shows that after a correction for this difference all REE abundances, except for Dy, would be the same for γ Equ and for HR 178 within the rms errors. This comparison supports Magazzu & Cowley's (1986) conclusion about the similarity of the REE abundance pattern in cool Ap and in Am stars. The large Dy overabundance has been confirmed with three Dy III lines at λ4207.816 (W_λ=23 mÅ), λ4685.801 (W_λ=5 mÅ), and λ4743.382 (W_λ=3 mÅ). Dy III lines were identified in the spectra of five other Ap stars by Aikman et al. (1979). The wavelengths of the Dy III lines just mentioned were taken from this paper. Eu is more abundant in α Cir (Paper I) and in HD 203932 (Paper II) than in γ Equ, but no corrections for possible magnetic and hyperfine-structure effects were made in the abundance analysis of those two stars.

6.5. Heavy elements U and Th

Adelman (1973) identified λ3859.6 Å as a U II line. His large uranium abundance of log(U/H) = -10.68 was not confirmed by U II lines in the 2000–3000 Å region by Faraggiana (1989). Cowley & Arnold (1978) were the first to propose Cr I λ3859.59 Å as identification of the observed feature, but a log(gf) = -1.48, which was used by the authors, was inconsistent with the observed equivalent width. A log(gf) = -0.017 for the Cr I line taken from Kurucz' GFIRON list (which also is contained in VALD) results in a slightly larger equivalent width than is observed for this line in γ Equ, thus indicating that the feature is totally due to Cr I and does not contain U II. Our calculations, together with the results by Faraggiana (1989), resolve the controversy concerning a large uranium overabundance in γ Equ.

Faraggiana (1989) was unable to derive the Th abundance with sufficient reliablility. We are in a similar position, because most of the Th II lines are severely blended. Synthetic spectra of the Th II λ4274.025 Å region give log(Th/H) = -10.30 (Fig. 5), and the other Th II lines contained in a region at λ4195.832 Å give $\log(\mathrm{Th}/\mathrm{N}_{tot})$ = -10.04. However, Th lines calculated with this abundance in other parts of our spectra have equivalent widths which are too large compared to the observations.

7. Conclusions

Three roAp stars with different observable magnetic fields (very small or zero in HD 203932, $B < 2$ kG in α Cir (Kupka et al. 1996), and $\approx$4.0 kG in γ Equ) show similar abundances in

their atmospheres. We improved the accuracy for the REE abundances, in particular for Eu, and confirm that the light elements have nearly solar abundances. From the iron peak elements, Co is overabundant by a factor of about 10 relative to the Sun. There is a tendency of an odd-even-violation in the sequence of Fe-Co-Ni, which can be also found for some s-process elements. Nb and Mo are the most overabundant elements in γ Equ relative to the Sun. Our calculations and observations clearly indicate that a large abundance for U, claimed in the literature, is entirely due to Cr I.

Finally, we contribute a further phase point to the magnetic field curve which has a period of nearly 80 years. Our analysis of line profiles of magnetic sensitive lines are in good agreement with a model proposed by Leroy et al. (1994), based on photopolarimetric observations. From a discussion of line profiles we have to conclude that the non-zero microturbulence values reported in the literature are artefacts due to magnetic field effects.

Similar to our previous papers on α Cir (Paper I) and HD 203932 (Paper II), we have to stress at this point that our analysis is based on a Kurucz ATLAS9 model atmosphere with scaled solar abundances which cannot provide a self consistent model for γ Equ, because of the obvious deviations in the abundance pattern discussed in this paper relative to the Sun. However, our preliminary results with model atmospheres which were computed with true abundances indicate that the corrections will be only of the order of the internal errors to the abundances derived in this paper.

Acknowledgements. This research was done within the working group *Asteroseismology-AMS*. The calculations were performed with an IBM RS6000-550 of the EDV-Zentrum der Universität Wien within the framework of the European Academic Supercomputer Initiative in connection with IBM, and with a DEC AXP-3000/600, funded through an DEC-EERP project (STARPULS). Research was supported by the Fonds zur Förderung der wissenschaftlichen Forschung (project *P 8776-AST*) and by a grant (95-02-06359) from the Russian Fond of Fundamental Researches. SJA's participation in this research was supported in part by grants from The Citadel Development Foundation. We thank Dr. Plachinda (Crimea) for providing us with observations, and we acknowledge usage of the SIMBAD database.

References

Adelman S.J. 1973, ApJS 26, 1
Adelman S.J., Bidelman W.P., Pyper D.M. 1979, ApJS 40, 371
Adelman S.J., Pyper D.M., Lopez-Garcia Z., Galiskan H. 1995, A&A 296, 467
Aikman G.C.L., Cowley C.R., Crosswhite H.M. 1979, ApJ 232, 812
Anders E., Grevesse N. 1989, Geochim. Cosmochim. Acta 53, 197
Babcock H.W., Cowling T.G. 1953, MNRAS 113, 357
Beavers W.I., Eitter J.J. 1986, ApJS 62, 147
Beckers J.M. 1969, "A Table of Zeeman Multiplets", AFCRL-69-0115, Physical Science Research Papers, No. 371
Biemont E., Baudoux M., Kurucz R.L., Ansbacher W., Pinnington E.H. 1991, A&A 249, 539
Biemont E., Hibbert A., Godefroid M., Vaeck N. 1993, ApJ 412, 432
Biemont E., Löwe R.M. 1993, A&A 273, 665
Biemont E., Quinet P., Zeippen C.J. 1993, A&AS 102, 435
Bizzarri A., Huber M.C.E., Noels A., Grevesse N., Bergeson S.D., Tsekeris P., Lawler J.E. 1993, A&A 273, 707
Bonsack, W.K., Pilachowski, C.A. 1974, ApJ, 190, 327
Corliss C.H., Bozman W.R. 1962, "Experimental Transition Probabilities for Spectral Lines of Seventy Elements", NBS Mono. 53, Washington, D.C.
Cowley C.R., Arnold C.N. 1978, ApJ 226, 420
Faraggiana R. 1989, A&A 224, 162
Gelbmann M., Kupka, F., Weiss W.W., Mathys G. 1997, A&A, in print (Paper II)
Hartoog M.R., Cowley C.R., Adelman S.J. 1974, ApJ 187, 551
Holweger H., Bard A., Kock A., Kock M., 1991, A&A 249, 545
Kupka F., Gelbmann M., Heiter U., Kuschnig R., Weiss W.W., Ryabchikova T. 1995, in "Astrophysical applications of stellar pulsation", ASP Conf. Ser. 83, 317
Kupka F., Ryabchikova T. A., Weiss, W.W., Kuschnig R., Rogl J., Mathys G. 1996, A&A 308, 886 (Paper I)
Kurtz D.W. 1983, MNRAS 202, 1
Kurucz R.L. 1993, Model atmosphere program ATLAS9 published on CDROM13
Kurucz R.L. 1994, Atomic Data for Mn and Co on CDROM21
Landi Degl'Innocenti E. 1975, A&A 45, 269
Leroy, J.L., Bagnulo S., Landolfi M., Landi Degl'Innocenti E. 1994, A&A 284, 174
Leroy J.L., Landolfi M., Landi Degl'Innocenti M., Landi Degl'Innocenti E., Bagnulo S., Laporte P. 1995, A&A 301, 797
Libbrecht K.G. 1988, ApJ 330, L51
Magazzu A., Cowley C.R. 1986, ApJ 308, 254
Martinez P., Weiss W.W., Nelson M.J., Kreidl T.J., Roberts G.R., Dorokhov N.I., Dorokhova T.N., Mkritichian D.E., Birch P.V. 1996, MNRAS, in print
Mathys G. 1990, A&A 232, 151
Mathys G. 1991, A&AS 89, 121
Mathys G., Lanz T. 1992, A&A 256, 169
Pinnington E.H., Ji Q., Guo B., Berends R.W., van Hunen J., Biemont E. 1993, Can. J. Phys. 71, 470
Piskunov N. E. 1992, in *"Stellar magnetism"*, eds. Yu.V. Glagolevskij & I.I. Romanyuk, Nauka, St. Petersburg, p. 92
Piskunov N. E., Kupka F., Ryabchikova T. A., Weiss W. W., Jeffrey C.S. 1995, A&AS 112, 525
Preston G. W. 1971, ApJ 164, 309
Renson P., Kobi D., North P. 1991, A&AS 89, 61
Rogl J. 1996, Master Thesis, University of Vienna, Austria
Seares F.H. 1913, ApJ 38, 99
Schneider H., Weiss W.W. 1989, A&A 224, 101
Scholz G. 1979, Astron. Nachr. 300, 213
Smirnov O.M., Piskunov N.E. 1994, in D.R. Crabtree, R.J. Hanisch & J. Barnes, eds, ASP Conf. Ser. 61, Astronomical Data Analysis Software And Systems III, Astron. Soc. Pac., San Francisco, p. 245
Smirnov O.M., Ryabchikova T.A. 1995, Astronomy Reports 39, 755
Thévenin F. 1989, A&AS 77, 137
van't Veer-Menneret C., Burkhart C., Coupry M.F. 1988, A&A 203, 123